

Wetting transitions in systems with van der Waals forces

C. Ebner, W. F. Saam, and A. K. Sen

Department of Physics, The Ohio State University, Columbus, Ohio 43210

(Received 31 January 1985)

Wetting and drying phase transitions in the presence of van der Waals forces are studied in the Ising lattice-gas model. With low-temperature series and mean-field analyses as a guide, a Landau theory, valid at temperatures below the bulk critical temperature T_c , is constructed. From the Landau theory, phase diagrams—including fourth-order, tricritical, critical, and critical end-point wetting transitions—are found. Fourth-order wetting occurs in the idealized case where substrate-adsorbate and adsorbate-adsorbate interactions differ only by an overall factor measuring relative strength. A scaling analysis is presented, and critical exponents, expected to be exact as hyperscaling predicts upper critical dimensions to be less than 3, are obtained. Detailed results from the full mean-field theory, in agreement with the Landau theory, are given, and in one case a detailed mapping from the mean-field theory to the Landau theory is provided. An exact symmetry between wetting and drying transitions, within mean-field theory, is found. The full mean-field equations, supplemented by a scaling analysis, are used to provide predictions of novel wetting and drying phenomena near T_c , as a function of variable adsorbate-adsorbate coupling near the adsorbate-substrate interface. Some of these phenomena bear resemblance to, but are distinct from, the special and extraordinary points which appear in the case of short-ranged forces. The relationship between the order of the transitions and the substrate and adsorbate potential parameters is systematically explored. Tuning of substrate-adsorbate interactions by plating the substrate with a monolayer of a third material is proposed as a means of producing critical wetting below T_c as well as, possibly, critical drying at T_c .

I. INTRODUCTION

Wetting transitions were predicted^{1,2} in 1977 and first observed³ in 1980. Since that time a large amount of theoretical^{4,5} and experimental³⁻⁶ work has been done in an effort to determine the conditions under which wetting (and drying⁵) transitions take place, the order of the transitions, and associated phase diagrams and critical properties. The nature of wetting transitions in systems with attractive long-range forces between adsorbate particles⁷ is the subject of considerable current interest.⁸⁻¹⁸ In this paper we examine the case of van der Waals attraction in some detail. We use Landau theory, mean-field theory, and scaling arguments to study, among other things, the wetting and drying phase diagrams as functions of the adsorbate-adsorbate and adsorbate-substrate potentials, the order of the various transitions, and the critical properties.¹⁹ Our basic theoretical model is the Ising lattice gas which was first used for multilayer adsorption calculations by de Oliveira and Griffiths.²⁰ This model has two bulk phases separated by a first-order phase transition ending at a critical point in the same manner as a real liquid-gas system. The principal difference between the behavior of the lattice model and a real fluid is the presence of layering and roughening transitions in the former at low temperatures but not the latter. Given appropriate caution when interpreting such transitions as they arise in the calculations, there is no difficulty in using the model for a fluid adsorbate. From low-temperature and mean-field studies of the model, we devise a continuum Landau theory from which the qualitative features of the wetting

(and drying) phase diagrams may be inferred. We construct appropriate scaling functions for the free energy at temperatures below²¹ the bulk adsorbate critical temperature T_c and determine the exponents associated with various critical wetting transitions. A hyperscaling argument¹³ is invoked to show that the upper critical dimension for each of these transitions is less than 3, and therefore the mean-field exponents are exact.

Comprehensive numerical solutions of the mean-field equations for the model are presented as well as an exact relationship between wetting and drying phase diagrams within mean-field theory. The mean-field calculations support the conclusions reached on the basis of the Landau theory and provide a detailed link between the substrate-adsorbate and adsorbate-adsorbate potential parameters and the parameters of the Landau theory. In addition, they provide predictions of novel wetting and drying phenomena close to T_c . The effect of enhanced or decreased adsorbate-adsorbate coupling in the vicinity of the adsorbate-substrate interface is examined in mean-field theory, especially in connection with wetting close to T_c . For enhanced coupling we find behavior not unlike, but distinct from, the results of Nakanishi and Fisher²² for surface-enhanced coupling in the case of purely short-range interactions. This behavior is further explored using scaling arguments.

The remainder of this paper is organized as follows. Section II contains a description of the lattice model, the mean-field equations, and the derivation of the relationship between wetting and drying phase diagrams. Further, the Landau theory is developed here from analytic

arguments including a low-temperature series expansion and approximate solution of the mean-field equations. Section III sets forth the results of the Landau theory including scaling functions and critical exponents, while Sec. IV presents detailed results of the mean-field calculations including comparison with the Landau theory and the description of wetting phenomena near T_c ; scaling arguments are developed for the latter. In Sec. V we examine systematically the relationship between the substrate and adsorbate potential parameters and the order of wetting transitions, arriving at general rules for choosing the adsorbate and substrate in such a way as to produce critical or first-order wetting. Finally, Sec. VI contains a summary.

II. MODEL

We begin this section with a description of the lattice-gas model for adsorption when long-range forces are present. The mean-field equations, analyzed in detail in Sec. IV, are given. From a low-temperature series and from the mean-field equations, a simple but very instructive Landau theory is developed.

We use the standard²⁰ Ising lattice-gas model of adsorption. The adatoms are allowed to occupy the sites of a point lattice located in the half-space $z > 0$. These sites are labeled i_m where m ($m \geq 1$) designates a net at constant z and i runs over the sites on this net. The Hamiltonian is

$$H = \sum_m \sum_{\langle i_m, j_m \rangle} W(i_m, j_m) t_{i_m} t_{j_m} + \sum_{m, m'} \sum_{i_m, j_{m'}} W(i_m, j_{m'}) t_{i_m} t_{j_{m'}} + \sum_m \sum_{i_m} (V_m - \mu) t_{i_m}, \quad (2.1)$$

where $\langle \rangle$ denotes a sum over distinct pairs, W is the interaction energy of a pair, V_m is the substrate potential in layer m , μ is the chemical potential, and $t_{i_m} = 0$ or 1 is the occupation number at site i_m .

The mean-field equations are written in terms of $n(m)$, the probability that a site in the m th layer is occupied, assuming that this probability depends only on the layer index m . It is convenient to introduce the quantities

$$w_{|n-m|} = \sum_{j_n} W(i_m, j_n) \quad (2.2)$$

and

$$W_n = \sum_{m (\geq n)} w_m. \quad (2.3)$$

In the sum for w_0 , the term $j_n = i_n$ is omitted. Notice

$$\Delta\Omega_w = \sum_{\substack{m, m' \\ m' < m}} [n(m)n(m') - n_\beta^2] (W_{m-m'} - W_{m-m'+1}) + \sum_m \frac{1}{2} w_0 [n^2(m) - n_\beta^2] + \sum_m (V_m - \mu_0 - \Delta\mu) [n(m) - n_\beta] + k_B T \sum_m \{ n(m) \ln n(m) + [1 - n(m)] \ln [1 - n(m)] - n_\beta \ln n_\beta - (1 - n_\beta) \ln (1 - n_\beta) \}. \quad (2.8)$$

Here, $\mu = \mu_0 + \Delta\mu$ where $\Delta\mu \leq 0$ to stabilize the bulk vapor phase. Next, we write the difference between the free energy

that W_n is the interaction energy between one adatom and a half-space of adatoms n layers away from the adatom; it is thus the natural analog of V_n .

The mean-field free energy is^{20,23}

$$\Omega = \sum_{\substack{m, m' \\ m' < m}} n(m)n(m') (W_{m-m'} - W_{m-m'+1}) + \sum_m \frac{1}{2} w_0 n^2(m) + \sum_m (V_m - \mu) n(m) + k_B T \sum_m \{ n(m) \ln n(m) + [1 - n(m)] \ln [1 - n(m)] \}. \quad (2.4)$$

Minimization of Ω with respect to $n(m)$ yields the mean-field equations

$$\sum_m n(m) (W_{|m-n|} - W_{|m-n|+1}) + w_0 n(n) + V_n - \mu = k_B T \ln \left[\frac{1 - n(n)}{n(n)} \right], \quad n = 1, 2, 3, \dots, \quad (2.5)$$

the term $m = n$ being omitted from the sum. In a real system, the interaction between adatoms is often altered²⁴ close to the substrate in comparison with its behavior in the bulk. We model this effect in a rough fashion by changing the coupling between adatoms in the first layer. Thus, in Eq. (2.4) we make the change

$$w_0 \rightarrow w_0 + (f - 1) w_0 \delta_{m,1} \quad (2.6)$$

with a corresponding change in Eqs. (2.5). In this way w_0 is replaced by $f w_0$ in the first layer of adsorbate.

The bulk mean-field equation may be recovered from (2.5) by setting all $V_m = 0$, letting the adatoms fill all space, and taking $n(m)$ independent of m . The result may be expressed as

$$n = 1 / (1 + e^{\beta(2\mu_0 n - \mu)}), \quad (2.7)$$

where $\mu_0 = W_1 + w_0/2$. For $T < T_c \equiv -\mu_0/2k_B$ there are two solutions n_α (liquid) and n_β (vapor) unless μ differs too much from μ_0 . These solutions have equal free energies at coexistence where $\mu = \mu_0$. Also, the high- (low-) density solution is stable for $\mu > \mu_0$ ($\mu < \mu_0$). At coexistence, $n_\alpha + n_\beta = 1$, whereas for $\mu \neq \mu_0$, $n_\alpha + n_\beta \neq 1$.

For this model, and in the mean-field approximation, there is a simple relationship between wetting and drying phase transitions and between the corresponding phase diagrams. We may expose the relationships by considering, first, the difference between the free energy of a film beneath bulk vapor and the free energy of a reference configuration with bulk vapor everywhere:

of a film beneath bulk liquid and the free energy of bulk liquid everywhere. We employ a different substrate potential V'_m and chemical potential $\mu' = \mu_0 + \Delta\mu'$:

$$\begin{aligned} \Delta\Omega_d = & \sum_{\substack{m, m' \\ m' < m}} [n'(m)n'(m') - n_\alpha'^2] (W_{m-m'} - W_{m-m'+1}) + \sum_m \frac{1}{2} w_0 [n'^2(m) - n_\alpha'^2] + \sum_m (V'_m - \mu_0 - \Delta\mu') [n'(m) - n_\alpha] \\ & + k_B T \sum_m \{ n'(m) \ln n'(m) + [1 - n'(m)] \ln [1 - n'(m)] - n_\alpha' \ln n_\alpha' - (1 - n_\alpha') \ln (1 - n_\alpha') \}. \end{aligned} \quad (2.9)$$

In this case, $\Delta\mu' > 0$ to stabilize the bulk liquid phase.

Now specify that $\Delta\mu' = -\Delta\mu$. Then from Eq. (2.7) one finds that $n_\alpha' = 1 - n_\beta$. Let us also define $n'(m) \equiv 1 - \delta(m)$ and use these relations to rewrite $\Delta\Omega_d$. The result is

$$\begin{aligned} \Delta\Omega_d = & \sum_{\substack{m, m' \\ m' < m}} [\rho(m)\rho(m') - n_\beta^2] (W_{m-m'} - W_{m-m'+1}) + \sum_m \frac{1}{2} w_0 [\rho^2(m) - n_\beta^2] + \sum_m (W_m - V'_m - \mu_0 - \Delta\mu) [\rho(m) - n_\beta] \\ & + k_B T \sum_m \{ \rho(m) \ln \rho(m) + [1 - \rho(m)] \ln [1 - \rho(m)] - n_\beta \ln n_\beta - (1 - n_\beta) \ln (1 - n_\beta) \}. \end{aligned} \quad (2.10)$$

If V_m and V'_m are such that $W_m - V'_m = V_m$, then Eq. (2.10) for $\Delta\Omega_d$ is the same as Eq. (2.8) for $\Delta\Omega_w$. Hence the drying phase diagram using this V'_m is identical to the wetting phase diagram using V_m provided the axes are scaled in the appropriate fashion. To take a specific example, used extensively in the numerical work presented in Sec. IV, let

$$w_0 = -2J, \quad W_m = -J/m^3, \quad (2.11)$$

and

$$V_m = -RJ \left[\frac{1}{m^3} + \sum_{p(\geq 4)} \frac{\gamma_p}{m^p} \right].$$

Then if

$$\begin{aligned} V'_m = W_m - V_m = & -J \left[\frac{1-R}{m^3} - R \sum_{p(\geq 4)} \frac{\gamma_p}{m^p} \right] \\ \equiv & -JR' \left[\frac{1}{m^3} + \sum_{p(\geq 4)} \frac{\gamma'_p}{m^p} \right], \end{aligned} \quad (2.12)$$

we find that the drying phase diagrams using $R' = 1 - R$, $\Delta\mu' = -\Delta\mu$, and $\gamma'_p = -R\gamma_p/(1-R)$ are identical to the wetting phase diagrams using R , $\Delta\mu$, and γ_p , provided the axes are scaled accordingly. Also, the densities $n'(m)$ in the drying case are the same as $1 - n(m)$, $n(m)$ being the density in the wetting case. We may conclude that for this model one need treat only wetting explicitly, the results for drying then being known. However, in the case of altered first-layer coupling, i.e., $f \neq 1$ in Eq. (2.6), there is no such simple relation between wetting and drying.

Many of the qualitative results found from detailed solution of the mean-field equations may also be obtained from a Landau theory whose derivation is now address. Consider first the slab approximation which, although very simple, contains an appreciable fraction of the physics of wetting transitions in the case of long-ranged forces.^{17,18} In this approximation the density is taken to be constant in the adsorbed film which is of thickness l as well as in the vapor above the film. The vapor density is taken to be n_β , the solution of the bulk equation (2.7). For the film's density we use the liquid density n_α .²⁵

Thus

$$n(m) = \begin{cases} n_\alpha, & m \leq l \\ n_\beta, & m > l. \end{cases} \quad (2.13)$$

Using Eq. (2.13) in Eq. (2.8), we find

$$\Delta\Omega_s = (n_\alpha - n_\beta) \sum_{m=1}^l (V_m - n_\alpha W_m) - (n_\alpha - n_\beta) l \Delta\mu, \quad (2.14)$$

where the subscript s refers to the slab approximation. If the adsorbate and substrate atoms interact via van der Waals potentials, then V_m and W_m will have leading terms of order m^{-3} at large m . Keeping, for the moment, just these terms, we write

$$W_m = -J/m^3, \quad V_m = -RJ/m^3, \quad (2.15)$$

and the l -dependent part of $\Delta\Omega_s$ is

$$\begin{aligned} \Delta\hat{\Omega}_s = & (n_\alpha - n_\beta) J (R - n_\alpha) \left[\frac{1}{2l^2} - \frac{1}{2l^3} + \frac{1}{4l^4} + O(1/l^6) \right] \\ & - (n_\alpha - n_\beta) l \Delta\mu. \end{aligned} \quad (2.16)$$

Consider this result at $\Delta\mu = 0$, for $\frac{1}{2} < R < 1$. Noting that n_α varies between 1 and $\frac{1}{2}$ as T goes from 0 to T_c , we see that if we define a temperature T_{cw} by

$$n_\alpha(T_{cw}) = R, \quad (2.17)$$

then, for $T < T_{cw}$, $\Delta\hat{\Omega}_s$ has a minimum at $l < \infty$, while for $T > T_{cw}$, there is a minimum at $l = \infty$. Thus T_{cw} is a possible wetting temperature. The transition, however, would be of infinite order in the slab approximation as at $T = T_{cw}$ and $\Delta\mu = 0$, there is no nonzero term to stabilize the free energy. Effects ignored in this approximation produce the desired stabilization. One way to obtain these is to perform a low-temperature series expansion of the free energy.¹⁸ A straightforward computation taking into account only single-particle or hole excitations in the ground state gives, at $\Delta\mu = 0$,

$$\Delta\Omega = \sum_{m=1}^l (V_m - W_m) - k_B T e^{\beta\mu_0} \times \left[\sum_{m=1}^{\infty} (e^{\beta(W_{l+m} - V_{l+m} - W_m)} - 1) + \sum_{m=1}^l (e^{\beta(V_{l-m+1} - W_{l-m+1} - W_m)} - 1) \right]. \quad (2.18)$$

The first term is from particle excitations in the gas above the film and the second, from holes in the film. At low T , $n_\beta = e^{\beta\mu_0} \ll 1$ so that T_{cw} is determined from $R = n_\alpha = 1 - e^{-\beta\mu_0}$. To describe wetting within the low- T series, T_{cw} must be small which requires that $1 - R$ be small and the differences $W_{l+m} - V_{l+m}$ and $V_{l-m+1} - W_{l-m+1}$ in the exponents in Eq. (2.18) may be neglected. To first order in n_β , $\Delta\Omega$ is thus

$$\Delta\Omega = \sum_{m=1}^l (V_m - W_m) - k_B T n_\beta \left[\sum_{m=1}^{\infty} (e^{-\beta W_m} - 1) + \sum_{m=1}^l (e^{-\beta W_m} - 1) \right], \quad (2.19)$$

of which the l -dependent part may be written as

$$\Delta\hat{\Omega} = - \sum_{m=l+1}^{\infty} [V_m - W_m - k_B T n_\beta (e^{-\beta W_m} - 1)]. \quad (2.20)$$

For l sufficiently large we may expand the exponential and find

$$\Delta\hat{\Omega} = - \sum_{m=l+1}^{\infty} \left[V_m - n_\alpha W_m - n_\beta \frac{\beta W_m^2}{2} + \dots \right]$$

$$\Delta\hat{\Omega}_s = (n_\alpha - n_\beta) J \left[(R - n'_\alpha) \left(\frac{1}{2l^2} - \frac{1}{2l^3} + \frac{1}{4l^4} \right) + \gamma_{w4} (RR_4 - n_\alpha) \left(\frac{1}{3l^3} - \frac{1}{2l^4} + \frac{1}{3l^5} \right) + \gamma_{w5} (RR_5 - n_\alpha) \left(\frac{1}{4l^4} - \frac{1}{2l^5} \right) + \gamma_{w6} (RR_6 - n_\alpha) \frac{1}{5l^5} + O(1/l^6) \right] - (n_\alpha - n_\beta) l \Delta\mu. \quad (2.24)$$

In the event that the substrate-adsorbate and adsorbate-adsorbate interactions differ only by an overall factor, all R_p are unity and the free energy is stabilized by the same $1/l^5$ term as in Eq. (2.21). More generally, if the R_p are not unity, additional corrections occur beginning in order $1/l^3$, as a consequence of adjustments to the densities $n(m)$ produced by all $R_p \neq 1$; this point is discussed in more detail in Sec. IV. In all cases explored using the full mean-field equations no indication was found that stabilization beyond the $1/l^5$ term is required.

On the basis of the preceding analysis as well as numerical solutions of the mean-field equations, we conclude that an appropriate form for $\Delta\Omega(l)$ for all $T < T_c$ is

$$\Delta\hat{\Omega}(l) = \frac{a_2}{2l^2} + \frac{a_3}{3l^3} + \frac{a_4}{4l^4} + \frac{a_5}{5l^5} - l(n_\alpha - n_\beta) \Delta\mu. \quad (2.25)$$

or

$$\Delta\hat{\Omega} = J(R - n_\alpha) \left[\frac{1}{2l^2} - \frac{1}{2l^3} + \frac{1}{4l^4} + O(1/l^6) \right] + \beta n_\beta J^2 / 10l^5 \quad (2.21)$$

if we use Eq. (2.15) for the potentials. Hence we find at low T that $\Delta\Omega(l)$ is stabilized by a term of order $1/l^5$ as a consequence of smoothing the slab profile²⁶ by thermal effects. The same result is found by taking $n(m) = n_0(m) + \Delta n(m)$ where $n_0(m) = n_\alpha$, $m \leq l$ and $n_0(m) = n_\beta$, $m > l$, and minimizing the mean-field free energy, Eq. (2.4) after linearizing the adsorbate-adsorbate interaction energy in Δn .²⁷ The same functional form of $\Delta\hat{\Omega}$ is found by carrying this calculation to the next order analytically and also results from our numerical studies of the mean-field equations at all temperatures examined.

Now generalize the interactions (2.15) to

$$W_m = -J \left[\frac{1}{m^3} + \sum_{p(\geq 4)} \frac{\gamma_{wp}}{m^p} \right]$$

and

$$V_m = -RJ \left[\frac{1}{m^3} + \sum_{p(\geq 4)} \frac{\gamma_{vp}}{m^p} \right]. \quad (2.22)$$

Furthermore, introduce

$$R_p \equiv \frac{\gamma_{vp}}{\gamma_{wp}}. \quad (2.23)$$

Then in the slab approximation, Eq. (2.16) is replaced by

Equation (2.25) provides us with a simple, yet very rich, Landau theory for wetting transitions. An analogous expression valid in the drying regime is obtained by interchanging n_β and n_α . Note that the Landau theory is a continuum theory and hence does not possess the discrete layering transitions present in the lattice-gas model.

III. LANDAU THEORY: RESULTS AND SCALING

In this section we analyze in detail the Landau theory developed above. At the outset we point out two differences between the Landau theory and the full mean-field theory, Eqs. (2.4) and (2.5). First, the Landau theory is incapable of dealing with phenomena at or near T_c , i.e., phenomena involving bulk correlation lengths comparable to or larger than the film thickness l . Second, as noted

briefly in the preceding section, for potentials of the general form (2.22), the coefficients a_3 and a_4 of Eq. (2.25) are not given precisely by Eq. (2.24); this point is discussed more fully in Sec. IV. Similarly, a_5 is not given exactly by Eq. (2.24) plus the profile correction appearing in Eq. (2.21). Except very near T_c , these differences are not important and the predictions of the Landau theory are substantially in agreement with those of the full mean-field theory except for quantitative details. Further, the Landau theory provides a more convenient vehicle for discussing scaling analytically.

The parameter space for the Landau theory is unrestricted but for the stabilization requirement $a_5 > 0$. As we focus on wetting, we have $n_\alpha - n_\beta > 0$ and $\Delta\mu \leq 0$. At $\Delta\mu = 0$, a variety of different critical wetting transitions occur, all signaled by the vanishing of $a_2 = (n_\alpha - n_\beta)J[R - n_\alpha(T)]$, at temperature T_{cw} defined by Eq. (2.17), i.e., $n_\alpha(T_{cw}) = R$. We turn now to discussion of the critical points.

A. Fourth-order critical wetting

When a_2 , a_3 , and a_4 simultaneously vanish at $\Delta\mu = 0$, fourth-order critical wetting occurs. This is an important special case which arises when $V_m = RW_m$, i.e., when the substrate-adsorbate and adsorbate-adsorbate potentials are identical except for overall strength. Minimization of $\Delta\hat{\Omega}$, Eq. (2.25), leads directly to the appropriate scaling form. We find, letting

$$(n_\alpha - n_\beta)\Delta\mu \equiv \Delta\tilde{\mu}, \quad (3.1)$$

$$\Delta\Omega = \tilde{t}^{2-\alpha_s} F_4 \left[\frac{a_3}{\tilde{t}^{\Delta_3}}, \frac{a_4}{\tilde{t}^{\Delta_4}}, \frac{\Delta\tilde{\mu}}{\tilde{t}^\Delta} \right],$$

in which $\tilde{t} = a_2$, $\alpha_s = \frac{1}{3}$, $\Delta_3 = \frac{2}{3}$, $\Delta_4 = \frac{1}{3}$, and $\Delta = 2$; the function $F_4(X, Y, Z)$ is

$$F_4(X, Y, Z) = \frac{1}{2g^2} + \frac{X}{3g^3} + \frac{Y}{4g^4} + \frac{a_5}{5g^5} - Zg, \quad (3.2)$$

where $g(X, Y, Z)$ is the solution of

$$g^3 + Xg^2 + Yg + a_5 + Zg^6 = 0. \quad (3.3)$$

From $\partial^2(\Delta\Omega)/\partial(\Delta\tilde{\mu})^2$ at $\Delta\mu = 0$ we find the scaling relation $2\nu_s = 2\Delta + \alpha_s - 2$ for the correlation length exponent; thus $\nu_s = \frac{7}{6}$. Following Lipowsky¹³ we find the upper critical dimension d_u from the hyperscaling relation $2 - \alpha_s = \nu_s(d_u - 1)$; it is $d_u = \frac{17}{7}$. As $d_u < 3$, we expect the mean-field exponents to be exact. Letting the equilibrium value l_0^{-1} of l^{-1} be the order parameter, and defining β_s by $l_0^{-1} \sim \tilde{t}^{\beta_s}$ at $\Delta\mu = 0$, we find from $\partial(\Delta\Omega)/\partial(\Delta\tilde{\mu})$ that $\beta_s = \Delta - 2 + \alpha_s = \frac{1}{3}$. Table I presents the exponents and upper critical dimension for this transition as well as for the others discussed below.

B. Tricritical wetting

If a_2 and a_3 simultaneously vanish at $\Delta\mu = 0$ while $a_4 > 0$, tricritical wetting is the result. In this instance we may ignore the a_5/l^5 term in $\Delta\Omega(l)$ and find

$$\Delta\Omega = \tilde{t}^{2-\alpha_s} F_3 \left[\frac{a_3}{\tilde{t}^{\Delta_3}}, \frac{\Delta\tilde{\mu}}{\tilde{t}^\Delta} \right], \quad (3.4)$$

in which $\tilde{t} = a_2$, $\alpha_s = 0$, $\Delta_3 = \frac{1}{2}$, and $\Delta = \frac{5}{2}$. Analysis of this case leads to $d_u = \frac{7}{3}$, $\nu_s = \frac{3}{2}$, and $\beta_s = \frac{1}{2}$.

C. Critical wetting

For critical wetting only $a_2 = 0$ at $\Delta\mu = 0$ and T_{cw} . The free energy is stabilized by $a_3 > 0$ and a_4 and a_5 may be ignored. Then

$$\Delta\Omega = \tilde{t}^{2-\alpha_s} F_2 \left[\frac{\Delta\tilde{\mu}}{\tilde{t}^\Delta} \right] \quad (3.5)$$

with $\tilde{t} = a_2$, $\alpha_s = -1$, and $\Delta = 4$. The upper critical dimension $d_u = \frac{11}{5}$ is again less than 3 and $\nu_s = \frac{5}{2}$ while $\beta_s = 1$.

D. Critical end points and associated critical points

If $a_3 > 0$ and $a_4 < 0$ (with $a_5 > 0$), critical wetting lines can end in critical end points. These occur when, at $a_2 = 0$, $\Delta\Omega$ has equal minima at $l = \infty$ and at some $l < \infty$. At such points $a_3 a_5 / a_4^2 = \frac{15}{64}$. Critical end points, if approached along a path such that l diverges continuously, have the same exponents as the critical wetting lines which they terminate. Associated with the critical end points (see the discussion of Figs. 1 and 2 below) are two-dimensional (2D) Ising critical points also occurring at $\Delta\mu = 0$. They are located at $a_4 = -\sqrt{3}a_3 a_5$, $a_2 = -a_3^{3/2} / 3\sqrt{3}a_5$, and have $l_0 = \sqrt{a_3} / 3a_5$.

E. Prewetting critical points

When there are first-order wetting transitions, there are associated prewetting^{1,2,4,28} lines which extend into the region $\Delta\mu < 0$ and terminate at critical points. These have mean-field critical exponents within our Landau theory and will have two-dimensional Ising exponents in general.

The various critical points are conveniently displayed in pictorial form. For a typical R , $\frac{1}{2} < R < 1$, Fig. 1 shows series of phase diagrams with different values of a_3 . The hatched sheets at $\Delta\mu = 0$ represent first-order transitions (bulk transitions) in which l_0 jumps from a finite value to infinity. The sheets curving down to the right are first-order prewetting surfaces, at which l_0 has a finite discontinuity, ending on prewetting critical lines (dashed). Figure 1(a) is for $a_3 = 0$. The line of dots at $a_2 = \tilde{t} = 0$ is a tricritical wetting line ending at a fourth-order critical point²⁹ O_4 . Along O_4A there is a first-order wetting. Near O_4 the line O_4A is described by $\tilde{t} \sim |a_4|^{1/\Delta_4} = |a_4|^3$. The prewetting critical line is described by $\tilde{t} \sim |a_4|^{1/\Delta_4}$ and $-\Delta\mu \sim |a_4|^{\Delta/\Delta_4} = a_4^6$. Figure 1(b) shows the case $a_3 > 0$. The tricritical line has become a second-order critical line (the usual critical wetting) terminating in the critical end point C_E . The prewetting critical line ends in the critical point C (associated with C_E in the sense described in Sec. III D above) which coexists with the bulk phase. Along CC_E , which also coexists with the bulk dense phase, there is a finite

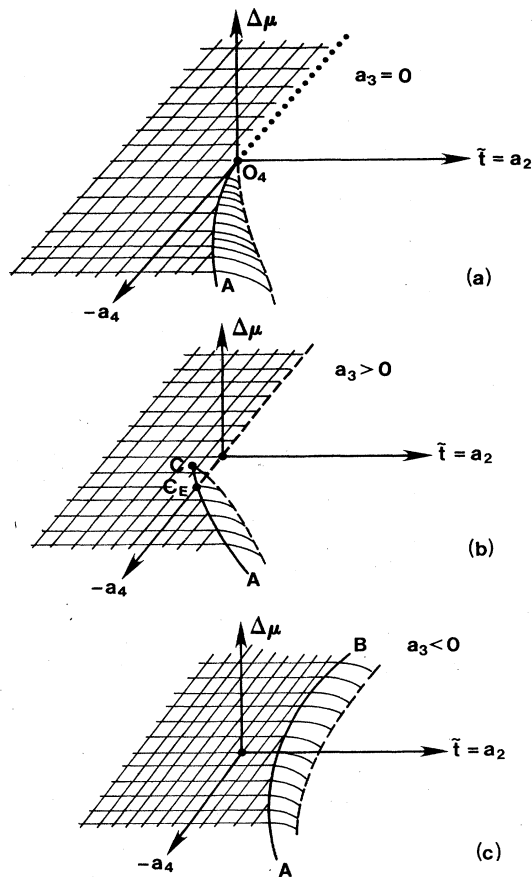


FIG. 1. Qualitative phase diagrams in a_4 - \tilde{t} - $\Delta\mu$ space for a typical R in the wetting regime $\frac{1}{2} < R < 1$ for (a) $a_3=0$, (b) $a_3 > 0$, (c) $a_3 < 0$. A detailed description is given in the text.

change in the film thickness as \tilde{t} is increased; the line from C_E to A is a line of ordinary first-order wetting transitions across which l_0 jumps from a finite value to infinity. For $a_3 < 0$, Fig. 1(c), there is only first-order wetting at $\Delta\mu=0$. Figure 2 shows a similar series of phase diagrams for various values of a_4 . Again, the hatched sheets at $\Delta\mu=0$ depict first-order bulk transitions, while the sheets curving down to the right are prewetting surfaces. Figure 2(a) is for $a_4=0$. The dashed line at $a_2=\tilde{t}=0$ is a critical wetting line terminating at the fourth-order point O_4 . Near O_4 the line O_4A is described by $\tilde{t} \sim |a_3|^{1/\Delta_3} = |a_3|^{3/2}$. The prewetting critical line is described by $\tilde{t} \sim |a_3|^{1/\Delta_4}$ and $-\Delta\mu \sim |a_3|^{\Delta/\Delta_4} = |a_3|^3$. Figure 2(b) shows the case $a_4 < 0$, and demonstrates again the critical end point and associated critical point of Fig. 1(b). For $a_4 > 0$, Fig. 2(c), there is a critical wetting line (dashed) at $\tilde{t}=0$ and $\Delta\mu=0$. This line terminates in the tricritical point O_3 . Along O_3A , described by $\tilde{t} \sim |a_3|^{1/\Delta_3} = |a_3|^2$, there is first-order wetting. The prewetting critical line is characterized near O_3 by $t \sim |a_3|^{1/\Delta_3}$, $-\Delta\mu \sim |a_3|^{\Delta/\Delta_3} = |a_3|^5$.

The information contained in Figs. 1 and 2 at $\Delta\mu=0$ is easily visualized in the plot of Fig. 3. There, AO_4 is a line of tricritical points ending in the fourth-order point O_4 .

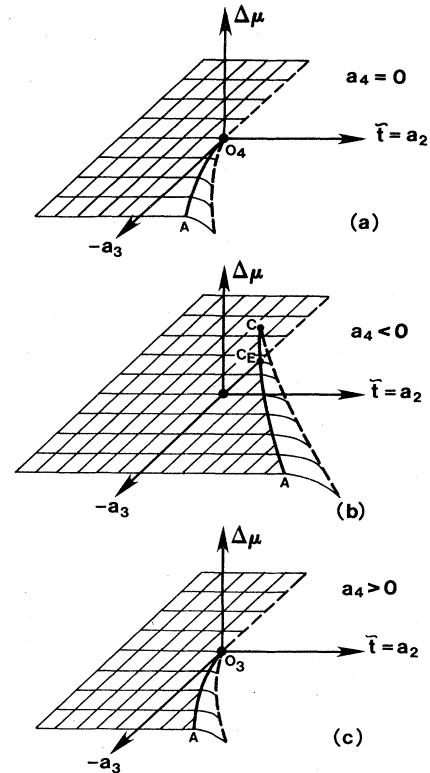


FIG. 2. Qualitative phase diagrams in a_3 - \tilde{t} - $\Delta\mu$ space for a typical R in the wetting regime $\frac{1}{2} < R < 1$ for (a) $a_4=0$, (b) $a_4 < 0$, and (c) $a_4 > 0$. A detailed description is given in the text.

At O_4 the tricritical line bifurcates into the critical end-point line O_4E [line of points C_E of Fig. 1(b)]; CO_4AB is a plane of critical wetting points at $\tilde{t}=0$. The wing EDO_4 extending to negative \tilde{t} is a first-order sheet at which there is a finite jump in l_0 . To the left and below CEO_4A is a first-order wetting sheet which curves towards positive \tilde{t} . Near O_4 , the line O_4E is described by $a_3 = 15a_4^2/64a_5$, i.e., $a_3 \sim a_4^{\Delta_3/\Delta_4}$ as noted in Sec. III D

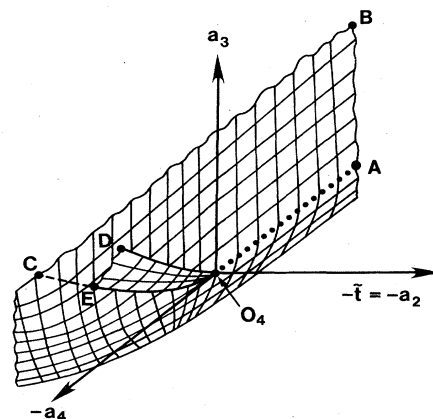


FIG. 3. Qualitative phase diagram in a_3 - a_4 - \tilde{t} space at gas-liquid coexistence ($\Delta\mu=0$) for a typical R in the wetting regime $\frac{1}{2} < R < 1$. A detailed description is given in the text.

while O_4D is given by $a_3 = a_4^2/3a_5$, $\tilde{\tau} = a_2(-|a_3|^{3/2}/27a_5^2)g$, i.e., $a_3 \sim a_4^{\Delta_3/\Delta_4}$ and $a_2 \sim a_4^{1/\Delta_4}$. The first-order sheet curving below the tricritical line AO_4 is composed of lines at constant a_4 which are described by $\tilde{\tau} \sim a_3^{1/\Delta_3} = a_3^3$.

The value of T_{cw} can be varied from 0 to T_c as R ranges from 1 to $\frac{1}{2}$. Although the Landau theory is unreliable for computing exponents for critical points at T_c as well as for a_4 too large and negative (as we shall see in Sec. IV), it is instructive to display its predictions as a function of R . In Fig. 4 we show an R - T - a_4 phase diagram for $a_3=0$. The curve AD is a line of fourth-order critical points, excepting point A . The sheet $ABCD$ is a tricritical sheet, excepting the line AB . This sheet is generated by sweeping the curve AD parallel to the a_4 axis; AD is determined by $R = n_\alpha(T)$. The sheet below AD is a surface of first-order wetting transitions. Under the assumptions that $a_2 = b_2[R - n_\alpha(T)]\Delta n$, $a_4 = -b_4\Delta n$, and $a_5 = \text{const}$, where $\Delta n = n_\alpha(T) - n_\beta(T)$ and b_2 and b_4 are constants, the temperature $T_w^{(1)}$ of the first-order sheet is determined by

$$\Delta n(T_w^{(1)}) = \frac{6^{3/2} a_5 b_2^{1/2} [R - n_\alpha(T_w^{(1)})]^{1/2}}{5 b_4^2},$$

where

$$l_0 = b_4 / \{6b_2[R - n_\alpha(T_w^{(1)})]\}^{1/2}.$$

For $\frac{1}{2} < R < 1$, then, $T_w^{(1)} \rightarrow T_c$ as $b_4 \rightarrow \infty$ since $\Delta n(T) \rightarrow 0$ as $T \rightarrow T_c$. Thus, the first-order wetting surface approaches T_c at large $|a_4|$. The full mean-field theory predicts that this surface actually reaches T_c at finite γ_4 , where drying phenomena come into play (see Sec. IV). Nevertheless, Fig. 4 is instructive for its many qualitatively correct features. We do not discuss the line AB as it is at T_c where the Landau theory completely breaks down. We have also found the full mean-field theory to be numerically intractable near AB as well.

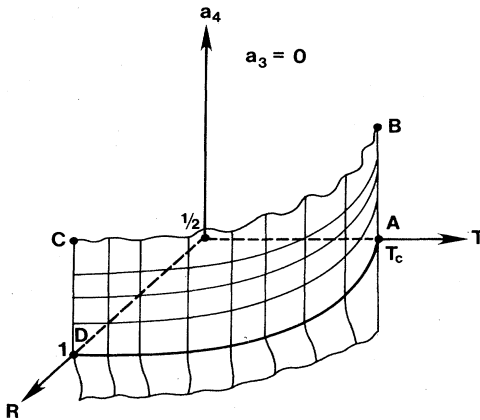


FIG. 4. Qualitative phase diagram in R - a_4 - T space at $a_3=0$ and at coexistence ($\Delta\mu=0$) for the full wetting regime $\frac{1}{2} < R < 1$. A detailed description is given in the text.

IV. NUMERICAL RESULTS

In this section we present results found from solving the mean-field equations (2.5) using potentials of the form (2.22). In regard to these potentials, preliminary calculations verified that the qualitatively important parameters are the relative values³⁰ $\gamma_{vp} - \gamma_{wp}$, and therefore most of the numerical work has been done using $\gamma_{wp}=0$ for all P . Thus we discuss here results obtained using

$$W_m = -J/m^3 \quad \text{and} \quad V_m = -RJ \left[\frac{1}{m^3} + \sum_{p \geq 4} \frac{\gamma_p}{m^p} \right], \quad (4.1)$$

where J is a positive constant. Notice that γ_{vp} is now written simply γ_p , which should not be ambiguous as all γ_{wp} are zero. Furthermore, we take

$$w_0 = -2J. \quad (4.2)$$

The numerical value of w_0 is quite unimportant with regard to the wetting and drying transitions. The value $-2J$ is convenient because then Eqs. (4.1) and (4.2) give $\mu_0 = -2J$ and, in mean-field theory, $k_B T_c = J$. Finally, as described in Sec. II, we will consider the effect of changing the coupling within the first layer only; specifically, we let the coupling within this layer become $w'_0 = -2fJ$, $f \neq 1$.

The mean-field equations were solved using anywhere from 30 to 300 layers of adsorbate, 120 layers being typical. The procedure employed was that of Ng³¹ in which one constructs the trial function for a given iteration in an optimum fashion from the outcomes of P previous iterations. We found the most rapid convergence to be obtained for $P=4$ or 5. For $T \leq 0.5T_c$, fewer than ten iterations were generally needed to produce convergence of all of the individual $n(m)$'s to within 10^{-12} . For $T \approx 0.999T_c$, several thousand iterations were generally required.

Extensive calculations have been done for wetting transitions as functions of R , T , $\Delta\mu$, γ_4 , f , and γ_5 , and for both wetting and drying transitions as functions of these parameters. We discuss first the work using $f=1$.

At $\Delta\mu=0$ one expects, and we find, wetting transitions for $\frac{1}{2} < R < 1$. At $\gamma_4 = \gamma_5 = 0$, there is fourth-order critical wetting which we were able to identify by showing numerically that $\beta_s = \frac{1}{3}$ as in the Landau theory of Sec. III. In the wetting regime with $\gamma_5=0$ and $\gamma_4 > 0$ we find ordinary critical wetting with $\beta_s=1$ (as in Table I) at T_{cw} such that $n_\beta(T_{cw}) = 1-R$. As can be seen³² from Eq. (2.24), this result is expected because a_4 should be positive for $\gamma_4 > 0$ [or $R_4 > 1$ in Eq. (2.24)] when $n_\alpha=R$. For $\gamma_5=0$ and $\gamma_4 < 0$, but not too large in magnitude, there is first-order wetting at some $T_w(\gamma_4) > T_{cw}$. As γ_4 becomes increasingly negative, $T_w(\gamma_4)$ approaches T_c , reaching this temperature at some value γ_{40} . At γ_{40} we apparently find a crossover from first-order wetting to a regime of critical drying at $\gamma_4 < \gamma_{40}$, the critical drying temperature being T_c . Let us now turn to detailed consideration of the phase diagrams.

Figure 5 shows wetting phase diagrams in γ_4 - T space at several values of R for $\gamma_5=0$ and $\Delta\mu=0$. For all R except 0.6, γ_{40} is too negative to appear on the figure; at

TABLE I. Critical exponents and upper critical dimension for the critical wetting transitions discussed in the text. For the prewetting critical line, including its end point C [see Fig. 1(b)], the exponents are those for Ising transitions in $d-1=2$ dimensions. Critical end points [C_E in Fig. 1(b)], if approached along a path such that l diverges continuously, have the same exponents as the critical wetting lines which they terminate.

Exponents	Wetting	Critical prewetting	Tricritical wetting	Fourth-order wetting
α_s	-1	$\alpha(d-1)$	0	$\frac{1}{3}$
Δ_1			$\frac{1}{2}$	$\frac{2}{3}$
Δ_2				$\frac{1}{3}$
Δ	4	$\Delta(d-1)$	$\frac{5}{2}$	2
β_s	1	$\beta(d-1)$	$\frac{1}{2}$	$\frac{1}{3}$
ν_s	$\frac{5}{2}$	$\nu(d-1)$	$\frac{3}{2}$	$\frac{7}{6}$
d_u	$\frac{11}{5}$	4	$\frac{7}{3}$	$\frac{17}{7}$

$R=0.6$, $\gamma_{40} \simeq -0.23$. The point on each curve at $\gamma_4=0$ is a fourth-order critical point separating a line (dashed) of critical wetting transitions from a line (solid) of first-order wetting transitions.

As shown in Sec. II, there are analogous drying phase transitions in the regime $0 < R' < \frac{1}{2}$. Specifically, there are phase diagrams identical to Fig. 5 given the reidentification of variables $R \rightarrow R' = 1 - R$ and $\gamma_4 \rightarrow \gamma'_4 = -\gamma_4 R / (1 - R)$. Further, the critical drying transition temperatures T_{cd} are such that $n_\alpha(T_{cd}) = 1 - R'$.

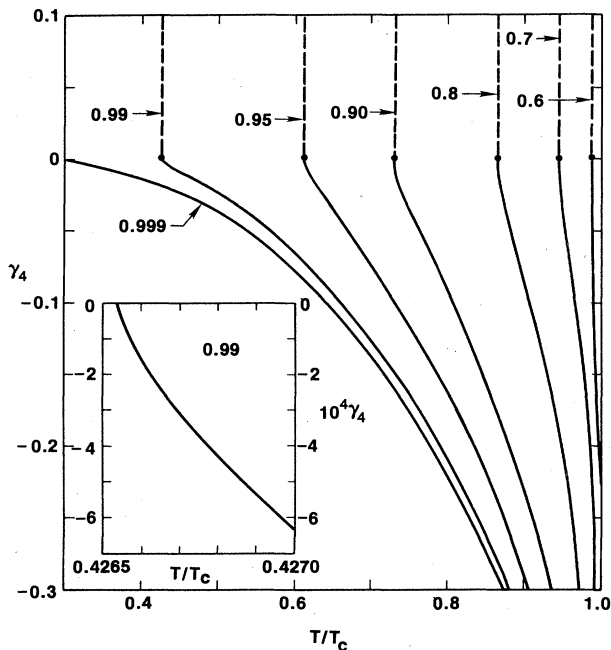


FIG. 5. Phase diagrams in γ_4 - T space for several values of R in the wetting regime with $\gamma_5=0$ and $\Delta\mu=0$. Each line of critical wetting transitions (---) is joined at $\gamma_4=0$ at a fourth-order critical point (●) to a first-order wetting line (—). The inset shows the first-order line at $R=0.99$ close to $\gamma_4=0$.

Suppose next that both γ_4 and γ_5 are nonzero. Then, for given R we shall examine the wetting transitions in the space of γ_4 , γ_5 , and T at $\Delta\mu=0$. Figure 6 shows at $R=0.99$ a set of wetting transition lines in γ_5 - T space at different values of γ_4 , while Fig. 7 shows the same in γ_4 -

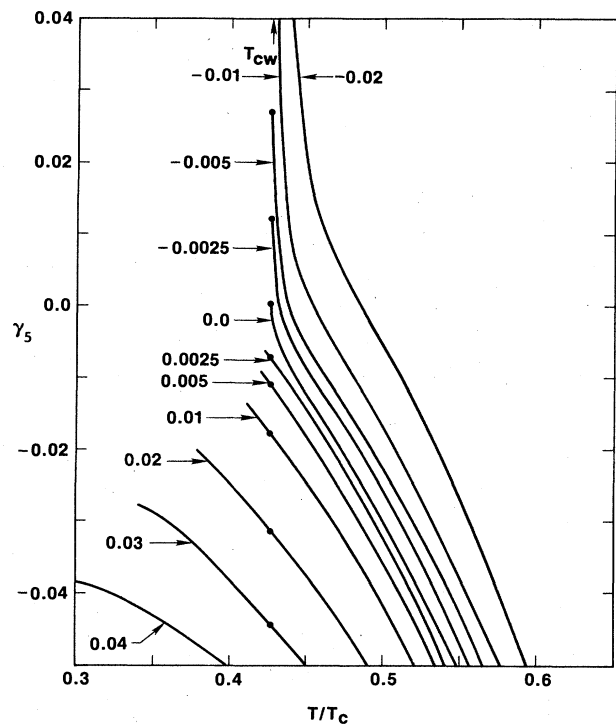


FIG. 6. Phase diagrams in γ_5 - T space for several values of γ_4 at $R=0.99$ and $\Delta\mu=0$. The lines shown are first-order wetting (at $T > T_{cw}$) or partial wetting (at $T < T_{cw}$) transitions. The line of critical wetting transitions (not shown) is at constant $T = T_{cw} = 0.4265T_c$ and is, for any given γ_4 , above the corresponding first-order line in the figure, terminating at the point where it intersects that line (●). For $\gamma_4 > 0$, this point is a critical end point; for $\gamma_4 < 0$, a tricritical point; and for $\gamma_4 = 0$, a fourth-order critical point.

T space at various values of γ_5 . Notice that the $\gamma_4=0$ line in Fig. 6 is much the same as the $\gamma_5=0$ line in Fig. 7. In both cases one finds ordinary critical wetting at positive gamma and first-order wetting at negative γ , with fourth-order critical wetting at $\gamma_4=\gamma_5=0$. We emphasize that in the case of $\gamma_4=0$ and $\gamma_5>0$ it is ordinary critical wetting and not tricritical wetting, because as mentioned in Sec. II, γ_5 contributes to the $a_3/3l^3$ term in the free energy.³³ This point is made graphically in Fig. 8 which displays lines of constant γ_4 and lines of constant γ_5 in a_3 - a_4 space for $R=0.99$, $\Delta\mu=0$, and $T=T_{cw}$ or $\tilde{t}=a_2=0$. These lines are at intervals $\Delta\gamma_4=0.02$ and $\Delta\gamma_5=0.10$. They were obtained by numerically fitting the mean-field free energy³⁴ as a function of film thickness to an expansion in inverse powers of the thickness and using Eq. (2.25) to define the a_p 's. The plane of the figure is the same as the $\tilde{t}=0$ plane of Fig. 3. Thus the origin is the fourth-order critical point, the positive a_4 axis is a line of tricritical points, etc. Note, in particular that if $\gamma_4=0$, $\gamma_5>0$ produces both $a_4>0$ and $a_3>0$ which is the regime of critical wetting.

Suppose now that γ_4 is fixed and negative. Then for γ_5 sufficiently large, a_3 and a_4 are positive and there is critical wetting. At some point, as γ_5 is decreased, a_3 crosses zero and a tricritical wetting transition is found. This se-

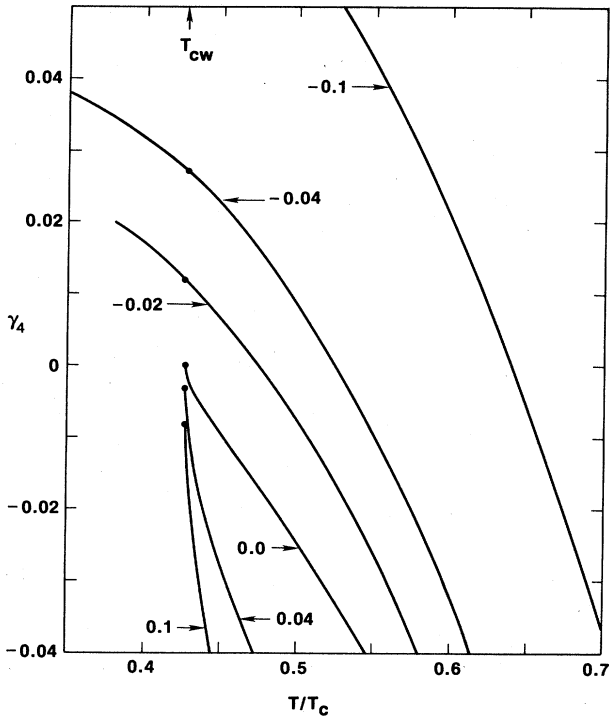


FIG. 7. Phase diagrams in γ_4 - T space for several values of γ_5 at $R=0.99$ and $\Delta\mu=0$. The lines shown are first-order wetting (at $T > T_{cw}$) or partial wetting (at $T < T_{cw}$) transitions. The line of critical wetting transitions (not shown) is at constant $T=T_{cw}=0.4265T_c$ and is, for any given γ_5 , above the corresponding first-order line in the figure, terminating at the point where it intersects that line (●). For $\gamma_5>0$, that point is a tricritical point; for $\gamma_5<0$, a critical end point; and for $\gamma_5=0$, a fourth-order critical point.

quence of events may be followed in Fig. 6 for e.g., the case of $\gamma_4=-0.005$. If $\gamma_5\geq 0.027$ there is critical wetting at T_{cw} ; if $\gamma_5\leq 0.027$ there is first-order wetting at $T_w > T_{cw}$; and at the crossover, there is a tricritical wetting point. A similar scenario unfolds by considering fixed $\gamma_5>0$ and γ_4 decreasing from some sufficiently positive value. The evolution of the wetting transition in this case may be traced on Figs. 7 and 8.

Quite different critical behavior results if γ_4 is fixed and positive or γ_5 is fixed and negative. In the first case, as γ_5 is decreased, a_3 will eventually vanish but only after a_4 has become negative. Then the line of critical wetting transitions is terminated by a critical end point; the line of critical phase transitions is met at this point by a line of first-order wetting transitions which continues to $T < T_{cw}$ as a partial wetting transition in which the coverage changes discontinuously from a film of a layer or so thickness to a thicker but still finite one.³⁵ This partial wetting line may end at some $T>0$, as in the case of $\gamma_4=0.03$ (see Fig. 6), or it may persist to $T=0$ as for $\gamma_4=0.04$. In the latter case, as $T\rightarrow 0$, the transition is just a glorified layering transition involving a jump from zero to two layers. Actually, at $\gamma_4=0.03$ also the partial wetting transition persists to $T=0$ as a pair of one-layer layering transitions which are inescapable in the Ising lattice-gas model. More realistically, it should end in a critical point as described in Sec. III. (See Ref. 35.) For γ_5 fixed and negative and varying γ_4 , similar behavior is found as depicted in Figs. 7 and 8. For each curve in Figs. 6 and 7, use of Fig. 8 allows construction of its image in Fig. 3.

In the drying regime, there is once again a perfect symmetry in that phase diagrams identical to those in the wetting regime are obtained under the transformation $R\rightarrow R'=1-R$, $\gamma_4\rightarrow\gamma'_4=-\gamma_4R/(1-R)$, $\gamma_5\rightarrow\gamma'_5=-\gamma_5R/(1-R)$, and wetting \leftrightarrow drying, as shown in Sec. II.

One expects that the addition of further terms to V_n of the form $-R\gamma_p/n^p$, $p>5$, will have much the same ef-

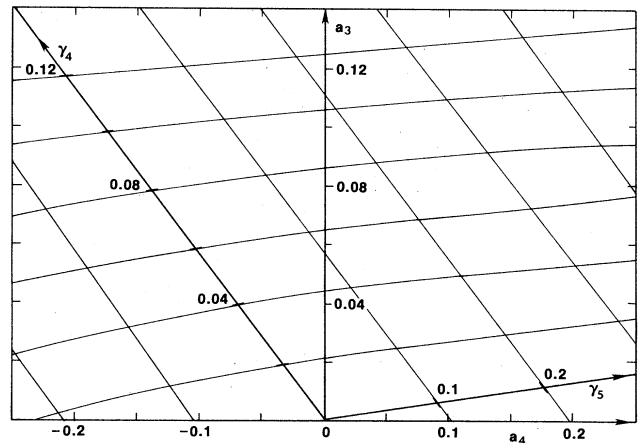


FIG. 8. Lines of constant γ_4 , at intervals $\Delta\gamma_4=0.02$, and lines of constant γ_5 , at intervals $\Delta\gamma_5=0.1$, are shown in a_3 - a_4 space at $R=0.99$, $T=T_{cw}$, and $\Delta\mu=0$. The a_3 - a_4 space is the same as the $\tilde{t}=0$ plane in Fig. 3.

fect as the term with $p=5$. As discussed in Ref. 33, the salient point regarding such terms is that they affect the part of the free energy that varies as $1/l^3$ through their effect on the density of the adsorbed film, and therefore lead to qualitatively the same phase diagrams and precisely the same critical exponents in general.

At $\Delta\mu \neq 0$ we find sheets (in γ_4 - T - $\Delta\mu$ space at fixed R and γ_5) of first-order prewetting (or predrying) transitions. Each sheet ends, at $\Delta\mu=0$, on one of the first-order lines discussed above (e.g., Fig. 7) and, at $\Delta\mu \neq 0$ on a line a prewetting critical points. This line of critical points terminates at the end of the first-order line at $\Delta\mu=0$, and it lies entirely at temperatures below T_c .³⁶ Mapped onto a_4 - T - $\Delta\mu$ space using the information in Fig. 8, they appear as sketched in Fig. 2 (for $T < T_c$; for T near T_c , see below). The prewetting sheets lie at $\Delta\mu < 0$, while the predrying sheets are at $\Delta\mu > 0$. The prewetting and predrying phase diagrams are identical under the transformation $R \rightarrow R' = 1 - R$, $\gamma_p \rightarrow \gamma'_p = -\gamma_p R / (1 - R)$, and $\Delta\mu \rightarrow \Delta\mu' = -\Delta\mu$.

The most striking feature of the prewetting (and, of course, the predrying) transitions is that they do not extend far from $\Delta\mu=0$ and $T=T_w$. For given potentials, the prewetting critical point is typically at $\Delta\mu_{cpw} \approx -0.001 k_B T_c$ and $T_{cpw} - T_w \approx 0.02 T_c$. The difference between the pressure at the prewetting critical point and that at gas-liquid coexistence at the same temperature is thus $\Delta P \approx n_\beta |\Delta\mu_{cpw}| \sim 10^{-3} n_\beta k_B T_c$, suggesting that the prewetting transitions lie so close to the bulk gas-liquid transition as to be very difficult to detect experimentally. It is worth noting that if the adsorbate particles interact only with nearest neighbors then the Ising lattice-gas model produces significantly longer³⁷ prewetting lines such that $\Delta\mu \approx -0.03 k_B T_c$. As real materials are more faithfully represented by the present model with van der Waals interactions, our results give some indication why prewetting transitions have been so elusive to experimentalists.

We turn next to results obtained using an altered coupling within the first layer which represents possible effects on the adsorbate-adsorbate coupling produced by the proximity of the substrate.²⁴ Within the mean-field theory, the altered coupling is represented by replacing w_0 for the first layer only by $f w_0$ with $f \neq 1$. Thus the contribution $w_0 N_1^2 / 2$ the free energy, Eq. (2.4), becomes $f w_0 N_1^2 / 2$ and the mean-field equations (2.5) are altered accordingly.

In what follows we shall keep $\gamma_5=0$ throughout. Figure 9 presents, for $R=0.99$, wetting phase diagrams at coexistence in the γ_4 - T plane for various values of f . For each value of f there is the usual critical wetting line (not shown for reasons of clarity) at T_{cw} running from positive γ_4 to its intersection with the appropriate line of first-order transitions. For $f > 1$, this intersection is a tricritical wetting point and the line of first-order wetting transitions terminates here.

The tricritical point moves toward negative γ_4 as f increases. In the regime of first-order wetting, T_w decreases with increasing f at fixed γ_4 . For $f < 1$, on the other hand, the critical line terminates at a critical end point at $\gamma_4 > 0$, while the first-order wetting line continues below

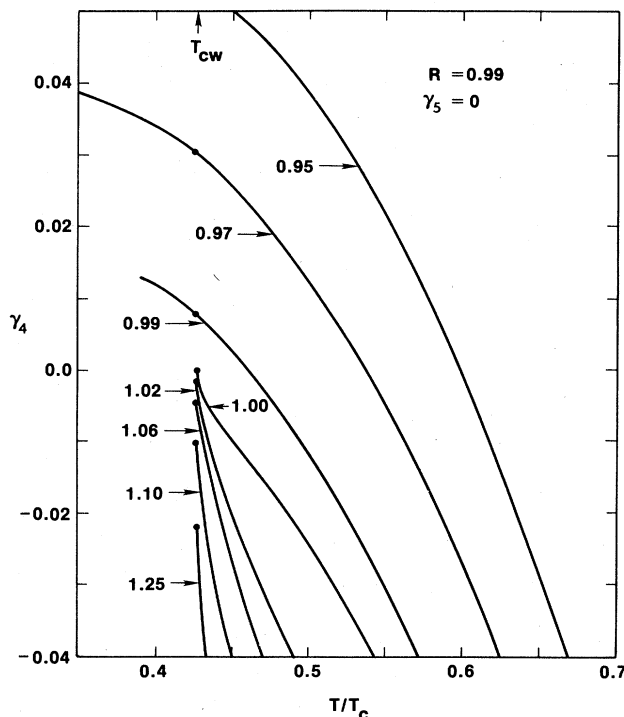


FIG. 9. Phase diagrams in γ_4 - T space for various values of f , the first-layer coupling enhancement factor, at $R=0.99$, $\gamma_5=0$, and $\Delta\mu=0$. The lines shown are first-order wetting (at $T > T_{cw}$) or partial wetting (at $T < T_{cw}$) transitions. The line of critical wetting transitions (not shown) is at constant $T=T_{cw}=0.4265 T_c$ and is, for any given f , above the corresponding first-order line in the figure, terminating at the point where it intersects that line (●). For $f > 1$, that point is a tricritical point, for $f < 1$, a critical end point; and for $f=1$, a fourth-order critical point.

T_{cw} as a partial wetting line. Overall, the phase diagram resembles Fig. 7 which is a γ_4 - T plot for $f=1$ but with various values of γ_5 . This fact is not surprising; an increased (decreased) coupling in the first layer or layers near the substrate is in some respects comparable to a short-ranged attractive (repulsive) substrate potential in that both would enlarge (depress) the density near the substrate, and therefore should have analogous effects on the free energies of films of a given thickness. Comparison of Figs. 7 and 9 shows that the foregoing is indeed true, at least for the case shown. At the same time, one expects that there must be other respects in which the two types of potential are not equivalent; a large f implies a raised critical temperature for any surface phase transition that may take place close to the substrate while a substrate potential $\sim \gamma_5/n^5$ will have no such consequences. This point is discussed further below.

Given $f \neq 1$, the phase diagrams in the drying regime $0 < R < \frac{1}{2}$ are similar to the wetting phase diagrams but there is no simple exact symmetry as in the case of $f=1$. We show in Fig. 10 the drying phase diagram at $\Delta\mu=0$ in γ_4 - T space for $R=0.01$ and $\gamma_5=0$ for several values of f . In the case of $f < 1$, the first-order drying lines become

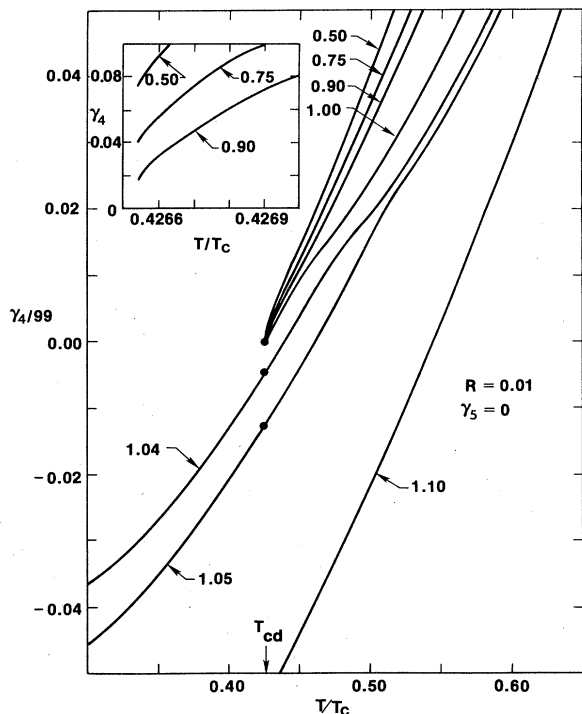


FIG. 10. Phase diagrams in γ_4 - T space at various values of f at $R'=0.01$ (in the drying regime), $\gamma_5=0$, and $\Delta\mu=0$. The vertical axis is $\gamma_4/99$, i.e., $(1-R')\gamma_4/R'$, to facilitate comparison with Fig. 9. The inset shows the region around $\gamma_4=0$ and $T=T_{cw}$.

critical drying lines at tricritical points located at values of $\gamma_4 > 0$; these values are very small and can be distinguished only in the inset. For $f > 1$, the critical drying line terminates at critical end points where the first-order drying transition becomes a partial drying transition.

The behavior of the wetting and drying transitions near the bulk critical temperature when $f \neq 1$ is quite interesting. Let us consider one particular case with $R > \frac{1}{2}$ in some detail, specifically, $R=0.9$. As γ_4 decreases toward some value $\gamma_{40}(R, f)$ the first-order wetting transition temperature T_w approaches T_c . For given R , γ_{40} is a decreasing function of f . For $\gamma_4 < \gamma_{40}$, there is, as stated earlier, no wetting transition. Rather, at T_c there is a critical drying transition, and, depending on f and γ_4 , a partial drying transition, in which the thickness of a gas film beneath bulk liquid changes discontinuously by an amount on the order of several atomic layers, may occur at $T < T_c$. The temperature of the latter transition increases with γ_4 and may or may not extend as high as T_c , depending on f . For $f < f_0$ ($f_0=1.60$ at $R=0.9$), the partial drying transition line ends at a critical point at some $\gamma_4 < \gamma_{40}$ and $T < T_c$. For $f > f_0$, the line ends at γ_{40} and T_c . In Fig. 11 the wetting and partial drying transitions are shown as solid lines in a γ_4 - T plot for $f=1.3$, 1.5, and 1.7. The dashed lines joining the lines of wetting transitions are partial wetting transitions, or surface transitions, in which the finite film's thickness jumps by several layers (from about zero to three or four layers).

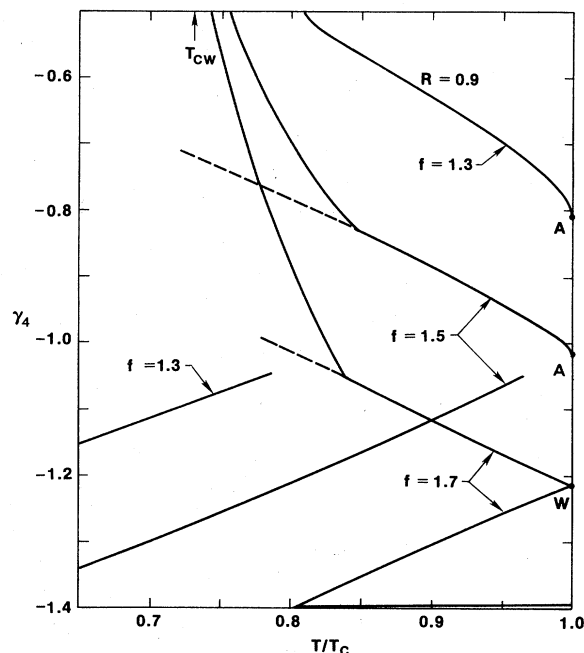


FIG. 11. Phase diagrams in γ_4 - T space for $f=1.3$, 1.5, and 1.7 at $R=0.9$, $\Delta\mu=0$, and $\gamma_5=0$. In each case, the first-order wetting lines intersect the line $T=T_c$ at some $\gamma_4=\gamma_{40}(f)$. For $f=1.7$, the wetting line meets a line of partial drying transitions at this point. In the cases of $f=1.3$ and 1.5, the partial drying line does not reach up to T_c but ends at a critical point at some $T < T_c$. The dashed lines at $f=1.5$ and 1.7 are lines of partial wetting transitions, each one intersecting the corresponding wetting line at a triple point and ending at a low-temperature critical point. Both the partial wetting and the partial drying transitions may be thought of as surface phase transitions brought about by the strongly enhanced first-layer coupling. Critical drying lines (not shown) extend downward from points A and W .

The line of these transitions, brought about by the enhanced adsorbate-adsorbate coupling near the surface, ends in a critical point, subject always to the caveat expressed earlier.³⁵

For each f , the critical drying transitions lie along a line (not shown for clarity) at T_c running from negative γ_4 up to the intersection with the line of wetting transitions at γ_{40} . The critical drying has been explored by studying the coverage Θ , defined by

$$\Gamma = \sum_m [n(m) - n_\alpha], \quad (4.3)$$

where n_α is the bulk liquid density, as a function of $t=(T_c-T)/T_c$ at fixed $\gamma_4 < \gamma_{40}$. We find that $|\Gamma|$ increases as t approaches zero; however, we cannot tell definitively from the numerical work whether or not it diverges at T_c because of convergence difficulties at $t \lesssim 0.002$. Any divergence that may appear at $T \rightarrow T_c$ is evidently quite weak, e.g., logarithmic. This is consistent with a scaling theory for the mean-field case; a more general scaling argument predicts a stronger divergence. We present the scaling argument shortly.

For $f=1.5$ and 1.7, the behavior of the wetting and

partial drying lines close to T_c and γ_{40} is shown in Fig. 12. Numerical analysis of these curves suggests strongly that $\Delta\gamma_4 = |\gamma_4 - \gamma_{40}| \sim t^{3/2}$ for the wetting line at $f > f_0$. For the partial drying line the analysis is less conclusive, but the results are quite consistent with the same exponent of $\frac{3}{2}$. As for the wetting line at $f < f_0$, analysis suggests $\Delta\gamma_4 \sim |t|^{1/2}$, but it is not particularly conclusive as we have been unable to approach much closer to T_c than $t=0.002$. At f_0 our numerical results (not shown) indicate that the wetting and partial drying lines join at T_c with slopes described by $\Delta\gamma_4 \sim t$. The critical point at T_c for this case will be called C . Those for the cases $f < f_0$ and $f > f_0$ will be labeled A and W , respectively, as indicated in Fig. 12.

The prewetting and pre-partial-drying phase-transition diagrams in the neighborhood of γ_{40} have quite different behavior depending on whether f is larger or smaller than f_0 . For $f < f_0$, the prewetting and pre-partial-drying sheets in γ_4 - T - $\Delta\mu$ space are separate and entirely at $T < T_c$. But for $f > f_0$, they become a single sheet extending to $T > T_c$. Figure 13(a) shows the γ_4 - T - $\Delta\mu$ plot at $R=0.9$ and $f=1.5 < f_0$; Fig. 13(b) is the corresponding phase diagram at $f=1.7 > f_0$. In the latter case, the prewetting and pre-partial-drying sheets are joined and extend to a maximum temperature of about $1.02T_c$. For still larger values of f , the sheet extends to higher temperature (e.g., to $T \approx 1.11T_c$ at $f=2$). In all cases, the critical line which forms the border of the prewetting wing ends at $\Delta\mu=0$ at the low-temperature end of the first-order wetting line unless this is at $T=0$.

We now turn to a scaling analysis of transitions near T_c . Our results are consistent with the idea that near T_c wetting and drying are controlled by bulk fluctuations. Consider first the critical drying of Figs. 11 and 12 occurring at T_c for $\gamma_4 < \gamma_{40}$. If we assume that $\Delta\Omega \sim \xi\Omega_b(t)$ where $\xi \sim t^{-\nu}$ is the bulk correlation length, we arrive at the Widom³⁸ scaling result $\alpha_s = \alpha + \nu$, where α and ν are bulk exponents. This may be rewritten as

$$\beta + \beta_s = \nu, \quad (4.4)$$

in which β is the bulk order-parameter exponent. Equation (4.4) states that near T_c , the film coverage $\Gamma = -\partial\Delta\hat{\Omega}/\partial\Delta\mu \equiv (n_\alpha - n_\beta)l_0 \sim t^{-\beta_s}$ diverges as

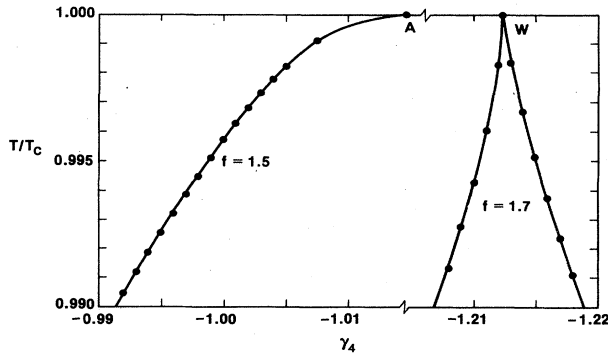


FIG. 12. Detail of the wetting and partial drying transitions close to T_c for $f=1.5$ and 1.7 . The dots (\bullet) are the mean-field results and the solid line is to guide the eye.

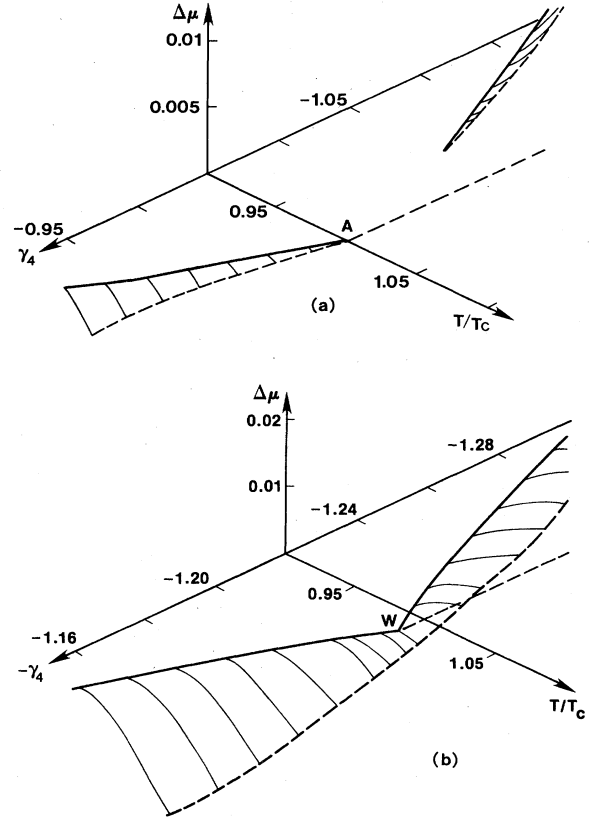


FIG. 13. Phase diagrams in γ_4 - $\Delta\mu$ - T space for $R=0.9$ and (a) $f=1.5$ or (b) $f=1.7$ at $\gamma_s=0$. The shaded regions at $\Delta\mu < 0$ and $\gamma_4 > \gamma_{40}$ are prewetting surfaces and those at $\Delta\mu > 0$ and $\gamma_4 < \gamma_{40}$ are pre-partial drying surfaces. For $f < f_0=1.60$, these surfaces are everywhere at $T < T_c$; for $f > f_0$, they extend above T_c . The dashed lines (---) are lines of critical drying transitions ending at points A (when $f < f_0$) and W (when $f > f_0$).

$$\Gamma \sim 1/t^{\nu-\beta}, \quad (4.5)$$

or, equivalently,

$$l_0 \sim t^{-\nu}. \quad (4.6)$$

Within mean-field theory $\nu = \beta = \frac{1}{2}$, so that $\Gamma \sim 1/t^0$, i.e., the divergence is at most logarithmic.³⁹ This is consistent with the numerical data reported above, and with the results of Nakanishi and Fisher²² for wetting and drying at T_c in the case of short-ranged potentials. The van der Waals potentials are hence not controlling the physics of transitions at T_c .⁴⁰

The argument leading to Eq. (4.5) should also apply for the transitions at the special points A , C , and W . Near these points $\Delta\Omega$ should scale, for fixed f , according to, if $\Delta\gamma_4 = \gamma_4 - \gamma_{40}$,

$$\Delta\hat{\Omega} = t^{2-\alpha_s} F \left[\frac{\Delta\gamma_4}{t^{\Delta_4}}, \frac{\Delta\tilde{\mu}}{t^{\Delta_s}} \right], \quad (4.7)$$

where the Widom result, $\alpha_s = \alpha + \nu$, should hold, and $\Delta_s = \Delta$, the bulk exponent. Our numerical data for the

first-order lines (noted above) then suggest that $\Delta_4 = \frac{1}{2}$ for A, 1 for C, and $\frac{3}{2}$ for W. Exponents for the various transitions at T_c are collected in Table II.

The transition at W is similar to the extraordinary transition of Nakanishi and Fisher.²² The exponents $\alpha_s = \alpha + \nu$ and $\Delta_s = \Delta$ are the same while their exponent $\Delta_1 = \frac{3}{2}$ for their surface field h , is the same as our $\Delta_4 = \frac{3}{2}$ for the field $\Delta\gamma_4$, which can be thought of as a surface field controlled by changing the van der Waals coupling between the adsorbate and the first substrate layer. The transitions are different, however, in that we have a partial drying line terminating at W in lieu of a drying line. Further, a critical drying line at T_c terminates at W; there is no analog of this line in the case of the extraordinary transition. The transition at C has the same similarities with and difference from the special point of Nakanishi and Fisher.²² The exponents α_s and Δ_s are the same, as is the surface field exponent. Once again both partial drying and critical drying lines terminate at C, possessing no analogs at the special point. Our additional relevant field at C, $\Delta f = f - f_0$, is physically the same as the enhancement of surface coupling field g in Ref. 22 at the special transition. For the case of short-ranged potentials there appears to be no analog of our critical point A.

The crucial difference between our work and that of Nakanishi and Fisher is, of course, the potential-range difference. In particular, for short-ranged potentials the surface field alone determines whether or not one has wetting or drying. For van der Waals potentials both γ_4 and R play this role. It is therefore not surprising that wetting and drying transitions are more complex in the van der Waals case. What is surprising is that the surface field exponents at C and W are (within numerical accuracy) the same as at the special and extraordinary points, at least within mean-field theory.

V. INTERACTIONS AND THEIR TUNING

In this section we study the forms of V_n and W_n within a model which possesses some important features of realistic physical systems. Our goal is to understand, in a

qualitative fashion, how to design an experimental system in which critical wetting phenomena may be observed. The model will allow the positioning of the adsorbate layers with respect to the substrate (the "excluded volume" effect) to be determined variationally. Our conclusion will be that the excluded volume effect is likely to produce first-order wetting, as in the work of Kroll and Meister.¹⁸ The model is then generalized to the case where the substrate is coated with a monolayer of a third material. Results indicate that an appropriately chosen coating can produce critical wetting.

We begin by introducing the "discrete layer model" in which the substrate atoms and adsorbate atoms are treated as being continuously distributed within discrete layers. The substrate layers are at $z' = -m'a_s$, $m' = 0, 1, 2, \dots$, while those of the adsorbate at $z = ma + \delta$, $m = 1, 2, \dots$. The distance δ is introduced to allow for the excluded volume effect; δ will be determined variationally by minimizing the substrate-adsorbate interaction energy.

Let a pair of atoms in the substrate interact via a Lennard-Jones (6-12) potential,

$$\phi_s(r) = 4\epsilon_s \left[\left(\frac{\sigma_s}{r} \right)^{12} - \left(\frac{\sigma_s}{r} \right)^6 \right], \quad (5.1)$$

and a pair of adsorbate atoms, by a 6-12 potential ϕ_w with range and depth parameters σ_w and ϵ_w . Finally, a substrate atom and an adatom are assumed to interact via a 6-12 potential ϕ_v with parameters σ_v and ϵ_v ; we shall set $\sigma_v = (\sigma_s + \sigma_w)/2$.

Integration of ϕ_v over the m' layer of substrate atoms gives

$$v_{m,m'} = \frac{4\pi}{5} n_s \sigma_v^2 \epsilon_v \left[\left(\frac{\sigma_v}{m'a_s + ma + \delta} \right)^{10} - \frac{5}{2} \left(\frac{\sigma_v}{m'a_s + ma + \delta} \right)^4 \right]; \quad (5.2)$$

$v_{m,m'}$ is the interaction energy of layer m' of the substrate with an adatom in layer m , given that n_s is the density of atoms in a layer of the substrate. The corresponding ex-

TABLE II. Critical exponents for transitions near T_c . The top entry in each case is the mean-field result, while the second entry is the expected exact result in terms of critical exponents for the Ising model in $d=3$ dimensions.

Exponents	Critical drying	A	C	W
α_s	$\frac{1}{2}$ $\alpha(d) + \nu(d)$	$\frac{1}{2}$ $\alpha(d) + \nu(d)$	$\frac{1}{2}$ $\alpha(d) + \nu(d)$	$\frac{1}{2}$ $\alpha(d) + \nu(d)$
Δ_s	$\frac{3}{2}$ $\Delta(d)$	$\frac{3}{2}$ $\Delta(d)$	$\frac{3}{2}$ $\Delta(d)$	$\frac{3}{2}$ $\Delta(d)$
Δ_4	$\frac{3}{2}$	$\frac{1}{2}$	1	$\frac{3}{2}$
β_s	0 $\nu(d) - \beta(d)$	0 $\nu(d) - \beta(d)$	0 $\nu(d) - \beta(d)$	0 $\nu(d) - \beta(d)$
ν_s	$\frac{3}{4}$ $\nu(d)$	$\frac{3}{4}$ $\nu(d)$	$\frac{3}{4}$ $\nu(d)$	$\frac{3}{4}$ $\nu(d)$

pression for the interaction energy of an adatom with a layer of adatoms m layers away is

$$w_m = \frac{4\pi}{5} n_a \sigma_w^2 \epsilon_w \left[\left(\frac{\sigma_w}{am} \right)^{10} - \frac{5}{2} \left(\frac{\sigma_w}{am} \right)^4 \right], \quad (5.3)$$

where n_a is the atomic number density in a layer of adsorbate. The total substrate potential in layer m , V_m , and the analogous quantity within the adsorbate, W_m , are

$$V_m = \sum_{m'=0}^{\infty} v_{m,m'}, \quad \text{and} \quad W_m = \sum_{m'=0}^{\infty} w_{m+m'}. \quad (5.4)$$

Noting that

$$\sum_{m'=0}^{\infty} \frac{1}{(m'+K)^4} = \frac{1}{3} \left[\frac{1}{K^3} + \frac{3/2}{K^4} + \frac{1}{K^5} + O(1/K^6) \right], \quad (5.5)$$

we find, for large m ,

$$W_m = -\frac{2\pi}{3} n_a \sigma_w^2 \epsilon_w \left(\frac{\sigma_w}{a} \right)^4 \times \left[\frac{1}{m^3} + \frac{3/2}{m^4} + \frac{1}{m^5} + O(1/m^6) \right], \quad (5.6)$$

while

$$V_m = -\frac{2\pi}{3} n_s \sigma_v^2 \left(\frac{\sigma_v}{a} \right)^4 \frac{a}{a_s} \times \left[\frac{1}{(m+\delta/a)^3} + \frac{3a_s/2a}{(m+\delta/a)^4} + \frac{(a_s/a)^2}{(m+\delta/a)^5} + O(1/m^6) \right]. \quad (5.7)$$

The latter may be expanded in powers of δ/ma to give

$$V_m = -\frac{2\pi}{3} n_s \sigma_v^2 \epsilon_v \left(\frac{\sigma_v}{a} \right)^4 \frac{a}{a_s} \times \left[\frac{1}{m^3} + \frac{3(a_s/2-\delta)/a}{m^4} + \frac{(a_s^2-6a_s\delta+6\delta^2)/a^2}{m^5} + O(1/m^6) \right]. \quad (5.8)$$

From Eqs. (2.22), (2.23), (5.6), and (5.8), we find

$$R = \frac{n_s \epsilon_v \sigma_v^6}{n_a \epsilon_w \sigma_w^6} \left(\frac{a}{a_s} \right), \quad (5.9)$$

$$\gamma_{v4} = 3(a_s/2-\delta)/a, \quad \gamma_{w4} = \frac{3}{2},$$

$$\gamma_{v5} = (a_s^2-6a_s\delta+6\delta^2)/a^2, \quad \gamma_{w5} = 1$$

and

$$R_4 = (a_s - 2\delta)/a, \quad (5.10)$$

$$R_5 = (a_s^2 - 6a_s\delta + 6\delta^2)/a^2.$$

Let us now introduce a value δ_0 of δ arrived at by the purely geometrical consideration, $a + \delta_0 = \frac{1}{2}(a_s + a)$, or

$$\delta_0 = \frac{1}{2}(a_s - a). \quad (5.11)$$

The excluded volume effect is naturally defined with respect to δ_0 . If $\delta > \delta_0$, the adsorbate is at a greater distance from the substrate than one would naively expect; there is a volume near the substrate from which the adsorbate is excluded. If $\delta < \delta_0$, the opposite is true.

In terms of δ_0 , R_4 and R_5 of Eqs. (5.10) may be rewritten as

$$R_4 - 1 = -2(\delta - \delta_0)/a, \quad (5.12)$$

$$R_5 - 1 = \left[\frac{1}{2}(a^2 - a_s^2) - 6(\delta - \delta_0)a + 6(\delta - \delta_0)^2 \right] / a^2.$$

It is clear from Eqs. (2.24)–(2.25) that it is desirable to have $R_4 > 1$ at T_{cw} (where $R = n_a$) to observe critical wetting. From Eqs. (5.12), then, a positive excluded volume effect ($\delta > \delta_0$) will prevent critical wetting, leading to first-order wetting. A negative excluded volume effect ($\delta < \delta_0$) will lead to critical wetting if $R_5 - 1$ is not too negative.⁴¹

We have determined δ by minimizing the substrate-adsorbate interaction energy⁴²

$$U(\delta) = \sum_{m=1}^{\infty} V_m. \quad (5.13)$$

The results of this calculation are very close to those obtained by minimizing just the interaction energy of the first layer of adsorbate with the first layer of substrate, i.e., by minimizing $v_{1,0}$. The latter procedure gives

$$\delta/\sigma_s = \left[1 + \frac{\sigma_w}{\sigma_s} \left[1 - \frac{a}{\sigma_w} \right] \right] / 2; \quad (5.14)$$

δ/σ_s as found from Eq. (5.14) is typically about 0.02 larger than the value found by minimizing $U(\delta)$. Inaccuracies engendered by the use of Eq. (5.14) may be ignored given the qualitative nature of arguments based on the discrete-layer model. From Eqs. (5.14) and (5.10), we find

$$\delta - \delta_0 = (\sigma_s + \sigma_w - a_s - a)/2. \quad (5.15)$$

In most fairly-densely-packed materials one expects core parameters to be greater than lattice interplanar spacings. For example, if a is the spacing between (111) planes of atoms in an fcc structure at $T=0$, assuming a (6-12) interatomic potential, then $a = 0.89\sigma_w$. As a general rule, then, we expect, from Eq. (5.15), that $\delta - \delta_0 > 0$, i.e., that there is a positive excluded volume effect. Further, first-order wetting is to be expected, as observed experimentally.⁶

Consider next the generalization of the discrete layer model, a monolayer of a third material being put in place of the first substrate layer. Let the distance between this layer and the substrate be a_m and the distance between this layer and the adsorbate be $a + \delta$. After a modicum of

computation, we find that Eqs. (5.12) are replaced by

$$\begin{aligned} R_4 - 1 &= 2[-(\hat{\delta} - \delta_0) + (\hat{r}a_s - a_m)]/a \\ R_5 - 1 &= [\frac{1}{2}(a^2 - a_s^2) - 6a(\hat{\delta} - \delta_0) + 6(\hat{\delta} - \delta_0)^2 \\ &\quad + 6a_m(a_m - a_s) - 12(\hat{\delta} - \delta_0)(\hat{r}a_s - a_m) \\ &\quad + 6(a - a_s)(\hat{r}a_s - a_m)]/a^2, \end{aligned} \quad (5.16)$$

where $\hat{r} = n_m \epsilon_m \sigma_m^2 / n_s \epsilon_s \sigma_s^2$ measure the ratio of monolayer-adsorbate interactions to substrate-adsorbate interactions. Also, n_m is the density of monolayer atoms, and ϵ_m and σ_m are the parameters for the monolayer atom-adsorbate atom (6-12) potential.

A calculation such as that leading to Eq. (5.15) provides

$$\hat{\delta} - \delta_0 = \delta - \delta_0 + (\sigma_m - \sigma_s)/2, \quad (5.17)$$

$\delta - \delta_0$ being given by Eq. (5.15). Thus, if we choose monolayer molecules which are sufficiently smaller than the substrate molecules, we can arrange that $\hat{\delta} - \delta_0 < 0$. If the monolayer molecules attract the adsorbate more than do the substrate molecules as well, we can guarantee that $\hat{r}a_s - a_m > 0$. From Eqs. (5.16) we then have $R_4 > 1$. The same assumptions about the monolayer molecules, will, as we see from Eq. (5.16), tend to make $R_5 > 1$ as well, especially if $a > a_s$.

In this scenario the excluded volume effect is overcome and conditions for critical wetting are achieved. It may be possible in practice that one of these critical wetting criteria (e.g., $\hat{r}a_s - a_m > 0$) is sufficiently well satisfied that another (e.g., small monolayer molecules) need not be, the desired goal still being met.

It follows from the discussion here and that of Sec. IV that critical drying at T_c can perhaps be found by reversing one or both of the criteria leading to $R_4 > 1$, thus making γ_4 (in Sec. IV) sufficiently negative.

VI. SUMMARY

In this work we have studied the influence of realistic long-ranged forces on wetting (and drying) phenomena. For temperature below the bulk critical temperature T_c , our mean-field theory maps onto a simple Landau theory which yields a rich spectrum of critical wetting transitions, including fourth-order, tricritical, critical end-point, and second-order phenomena. A hyperscaling argument showed that the upper critical dimension for these transitions is in each case less than 3; the mean-field exponents are thus expected to be exact. The fourth-order wetting point, a key feature of the phase diagram in the relevant

space of couplings and temperature (see Fig. 3) is found for the simplest class of potentials, where the substrate-adsorbate and adsorbate-adsorbate interactions differ only by a single relative strength parameter.

A study of transitions at and near T_c as a function of varying first-layer coupling, using the full mean-field theory, yielded an interesting crossover from a first-order wetting regime to one of critical drying at T_c . Associated with this crossover are three apparently new kinds of critical points, the points *A*, *C*, and *W* of Sec. IV. Two of these points bear both striking similarities to, and striking differences from, the special and extraordinary points found for the case of short-ranged interactions.²²

A simple analysis of potentials (Sec. V) within a model possessing more realistic features of real systems than the pure lattice-gas model suggested why only first-order wetting has yet been observed. This analysis also suggested that critical wetting may be observable in nature by use of the device of plating the substrate with a layer (or perhaps layers) of a third material made of molecules whose most important property must be that they interact more strongly with the adsorbate than do the substrate molecules.

It is, of course, exceedingly unlikely that a system could be tailored so as to allow direct observation of fourth-order critical wetting. Nevertheless, second-order critical wetting seems within reach, and systems might be chosen so that the presence of critical end points as well as tricritical and fourth-order points might influence experimental results to the extent that data analysis should account for these phenomena.

The possibility of observing critical drying at T_c is very intriguing. This would most likely occur for the case where the substrate is plated with a material which attracts the adsorbate rather more weakly than does the substrate.

ACKNOWLEDGMENTS

We wish to thank the Aspen Center for Physics (Aspen, Colorado) for providing a stimulating environment where part of this work was done. Conversations there with M. E. Fisher, D. E. Sullivan, J. W. Cahn, B. Widom, and M. R. Moldover were very useful. Conversations with C. Jayaprakash concerning multicritical phenomena were crucial. Finally, we wish to thank M. Schick for useful conversations concerning the work in Ref. 17. This work was supported in part by National Science Foundation Grant No. DMR-84-04961.

¹C. Ebner and W. F. Saam, Phys. Rev. Lett. **38**, 1486 (1977).

²J. W. Cahn, J. Chem. Phys. **66**, 3667 (1977).

³M. R. Moldover and J. W. Cahn, Science **207**, 1073 (1980).

⁴D. E. Sullivan and M. M. Telo de Gama, in *Fluid Interfacial Phenomena*, edited by C. A. Croxton (Wiley, New York, 1985), give a thorough review of wetting transitions including many references to the relevant literature. Work prior to 1982 is reviewed in Ref. 5.

⁵R. Pandit, M. Schick, and M. Wortis, Phys. Rev. B **26**, 5112 (1982). Drying transitions were first predicted in this paper.

⁶Very recent work includes S. G. J. Mochrie, M. Sutton, R. J. Birgeneau, D. E. Moncton, and P. M. Horn, Phys. Rev. B **30**, 263 (1984); D. D. Awschalom, G. N. Lewis, and S. Gregory, Phys. Rev. Lett. **51**, 581 (1983); J. W. Schmidt and M. R. Moldover, J. Chem. Phys. **79**, 379 (1983); J. J. Hamilton and D. L. Goodstein, Phys. Rev. B **28**, 3838 (1983); J. Krim, J. G.

Dash, and J. Suzanne, Phys. Rev. Lett. **52**, 640 (1984); J. Suzanne, J. L. Sequin, M. Bienfait, and E. Lerner, *ibid.* **52**, 637 (1984).

⁷A long-range force between adsorbate and substrate is a common feature of much of the earlier theoretical work; such a force between a pair of adsorbate particles is not.

⁸C. Ebner, W. F. Saam, and A. K. Sen, Phys. Rev. B **31**, 6134 (1985). This paper contains a brief description of some of the work reported here.

⁹M. P. Nightingale, W. F. Saam, and M. Schick, Phys. Rev. Lett. **51**, 1275 (1983); Phys. Rev. B **30**, 3830 (1984).

¹⁰W. F. Saam, Surf. Sci. **125**, 253 (1983).

¹¹P. Tarazona and R. Evans, Mol. Phys. **48**, 799 (1983).

¹²R. Evans and P. Tarazona, J. Chem. Phys. **80**, 587 (1984).

¹³R. Lipowsky, Phys. Rev. Lett. **52**, 1429 (1984).

¹⁴R. Lipowsky and D. M. Kroll, Phys. Rev. Lett. **52**, 2203 (1984).

¹⁵G. F. Teletzke, L. E. Scriven, and H. T. Davis, J. Chem. Phys. **78**, 1431 (1983).

¹⁶E. H. Hauge, in *Fundamental Problems in Statistical Mechanics VI*, edited by E. G. D. Cohen (North-Holland, New York, 1985), p. 65.

¹⁷S. Dietrick and M. Schick, Phys. Rev. B **31**, 4718 (1985).

¹⁸D. M. Kroll and T. F. Meister, Phys. Rev. B **31**, 392 (1985).

¹⁹The Landau theory, scaling description, and critical exponents, given van der Waals forces, have been reported briefly in Ref. 8, along with a short qualitative discussion of the mean-field calculations. New in this paper are the complete mean-field results, the predictions of the wetting behavior close to the bulk adsorbate critical temperature, the derivation of the exact relationship between wetting and drying phase diagrams in the lattice-gas model and mean-field theory, the study of the effect on adsorption phenomena of enhanced or decreased adsorbate-adsorbate coupling near the substrate, the study of the dependence of the order of wetting transitions on the potential parameters in general, and the demonstration of the relationship in mean-field theory between the microscopic potential parameters and the parameters of the Landau theory.

²⁰M. J. de Oliveira and R. B. Griffiths, Surf. Sci. **71**, 687 (1978).

²¹That is, temperature such that the bulk correlation length is small compared to other relevant lengths in the system.

²²H. Nakanishi and M. E. Fisher, Phys. Rev. Lett. **49**, 1565 (1982).

²³C. Ebner, Phys. Rev. A **22**, 2776 (1980).

²⁴It is well known that a substrate modifies the van der Waals forces between adsorbed molecules in its vicinity. See, e.g., S. Rauber, J. R. Klein, and M. W. Cole, Phys. Rev. B **27**, 1314 (1983); A. D. McLachlan, Mol. Phys. **7**, 381 (1964).

²⁵Here we use the higher density (metastable) solution n_α of the bulk mean-field equation [Eq. (2.7)] for the liquid density $n(m)$ at $m \leq l$ when $\Delta\mu < 0$. With this prescription the expression for $\Delta\hat{\Omega}_s$ in Eq. (2.14) is valid at least through order $(\Delta\mu)^2$. The same prescription emerges from the low-temperature series formalism discussed later in Sec. II. At $\Delta\mu = 0$, of course, n_α is a stable solution of Eq. (2.7).

²⁶It is worth noting that in the low- T series the film profile is given by

$$n(m) = \begin{cases} 1 - n_\beta e^{-\beta(W_{l-m+1} + W_m - V_m)}, & m \leq l \\ n_\beta e^{-\beta(W_{m-l} + V_m - W_m)}, & m > l. \end{cases}$$

For $m \gg l$, the density varies as $W_{m-l} + V_m - W_m$, thus hav-

ing a van der Waals tail with contributions from both the film-vapor interface (via W_{l-m}) and the substrate-film interface (via $V_m - W_m$). Similar effects occur within the liquid film ($m < l$) where, if both m and $l - m$ are large, the density varies as $W_{l-m} + W_m - V_m$. Van der Waals tails in interfacial profiles in the absence of substrates have been noted previously; see, e.g., P. G. de Gennes, J. Phys. Lett. (Paris) **42**, L377 (1981).

²⁷In this approximation, at $\mu = \mu_0$ and for $V_m/W_m = R = n_\alpha$, the l -dependent part of the free energy is

$$\begin{aligned} \Delta\hat{\Omega} &= \frac{\beta n_\alpha n_\beta (n_\alpha - n_\beta)^2}{2} \sum_{m=l+1}^{\infty} W_m^2 \\ &= \frac{\beta n_\alpha n_\beta J^2 (n_\alpha - n_\beta)^2}{10} \frac{1}{l^5} + O(1/l^6), \end{aligned}$$

which may be compared with the corresponding term in Eq. (2.21). For general T, μ, V_m , and W_m the profile is

$$n(m) = \begin{cases} n_\alpha / \{ 1 + [(1 - n_\alpha)/n_\alpha] e^{\beta(V_m - n_\alpha W_m)} \\ \quad \times e^{-\beta(n_\alpha - n_\beta)W_{l-m+1}} \}, & m \leq l \\ n_\beta / \{ (1 - n_\beta) e^{\beta(V_m - n_\alpha W_m)} \\ \quad \times e^{\beta(n_\alpha - n_\beta)W_{m-l}} \}, & m > l. \end{cases}$$

For small n_β these expressions reduce to those from the low-temperature series analysis.

²⁸R. Pandit and M. Wortis, Phys. Rev. B **25**, 3226 (1982).

²⁹S. Krinsky and D. Mukamel, Phys. Rev. B **11**, 399 (1975).

³⁰For example, if all $\gamma_{vp} = \gamma_{wp}$, i.e., $V_m = RW_m$, we find the fourth-order critical wetting point discussed in Sec. III A; if then we make $\gamma_{vp} < \gamma_{wp}$ for one value of p , first-order wetting results, and if instead $\gamma_{vp} > \gamma_{wp}$ for one p , ordinary critical wetting results.

³¹K.-C. Ng, J. Chem. Phys. **61**, 2680 (1974).

³²At T_{cw} and $\Delta\mu = 0$, $n_\alpha = R$ and the coefficient of $1/l^3$ in Eq. (2.24) is $\gamma_{w4}(R_4 - 1)RJ/3$. In the present case, $\gamma_{w4} = 0$ and the coefficient reduces to $R\gamma_4/3$.

³³The origin of this term is as follows. Introduction of a contribution $\sim \gamma_p/m^p$ in V_s produces corresponding changes in all occupation numbers $n(m)$. These changes in the densities then give rise, via the adsorbate-adsorbate interaction $W_m \sim 1/m^3$, to a term in Ω of order $1/l^3$. Hence the production of the $1/l^3$ part of Ω will take place regardless of the value of p . Indeed, one need only change $n(1)$ to affect a_3 .

³⁴The existence of the first-order layering transitions (see Ref. 35) allows us to find $\Delta\Omega$ at many different film thicknesses l corresponding to metastable states of the model. It is then possible to fit $\Delta\Omega(l)$ to the appropriate power series.

³⁵In the Ising lattice-gas model, there are always layering transitions at low temperature in which the coverage changes by about one atomic layer. To distinguish these from the partial wetting transition we somewhat arbitrarily adopt the point of view that the latter involves a change in coverage by two or more layers. In our phase diagrams we do not show the layering transitions which in fact are present in all of our mean-field calculations except for those close to T_c . In a real fluid or a continuum model such as that discussed in Sec. III, one would expect that partial wetting transitions could certainly exist even though layering transitions are not the rule. Hence we feel that our interpretation of the numerical results is a reasonable one and faithfully reflects the underlying physics.

³⁶If the coupling within the adsorbate near the substrate is strongly enhanced, the behavior of the prewetting and predrying surfaces can be quite different. See the discussion below in Sec. IV.

³⁷A Monte Carlo study of one such case is given by C. Ebner, Phys. Rev. A **23**, 1925 (1981). Also, we have done a series of mean-field and Monte Carlo calculations studying the evolution of the prewetting line as a function of the range of the adsorbate-adsorbate interaction for $V_n \sim 1/n^3$. See A. K. Sen, Ph.D. thesis, Ohio State University, 1985.

³⁸B. Widom, J. Chem. Phys. **43**, 3892 (1965).

³⁹As noted earlier, in the numerical data we cannot distinguish whether Γ diverges logarithmically or merely approaches a constant. In the latter case there is no drying at T_c . However, if the correct Ising 3D exponents are inserted in Eq. (4.5), then $\Gamma \sim t^{-0.36}$, which certainly does diverge. Thus, we do have critical drying at T_c for $\gamma_4 < \gamma_{40}$.

⁴⁰The leading term in the free energy coming from van der Waals force will vary as $t^{\beta+2\nu}$, coming from the $(n_\alpha - n_\beta)/l^2$ term in $\Delta\hat{\Omega}$. Hyperscaling gives a contribution $\sim \xi^{-2} \sim t^{2\nu}$ to

$\Delta\hat{\Omega}$ coming from bulk fluctuations. Thus, in an exact theory fluctuations will dominate van der Waals forces near T_c . Within mean-field theory $\Delta\hat{\Omega}$ varies as $t^{2-\alpha_s} \sim t^{2-\alpha-\nu} = t^{3/2}$ from fluctuations. As $t^{\beta+2\nu} = t^{3/2}$, also, in mean-field theory, fluctuation and van der Waals effects are comparable. Note that for potentials of sufficiently long range, e.g., $1/z^2$ in place of $1/z^3$, leading to a term $\sim t^{\beta+\nu}$ in $\Delta\hat{\Omega}$, bulk fluctuations will *not* control the physics of wetting or drying at T_c , and exponents will depend on the potential range. A longer-ranged potential could be produced by charging the substrate, leading to monopole-induced dipole interatomic forces and a $1/z^2$ substrate-adsorbate potential.

⁴¹Negative $R_5 - 1$ will tend to make $a_4 < 0$. If, however, $a_3 > 0$, critical wetting may still occur, as in Fig. 3. Note also from Figs. 6 and 7 that one can have critical wetting with $\gamma_5 < 0$ if γ_4 is sufficiently positive.

⁴²In this calculation, the full (10-4) potentials, Eqs. (5.2) and (5.3), must be used in Eqs. (5.4) in order to include the essential short-range repulsion effects.